Carbohydrate Polymers 98 (2013) 50–63

Contents lists available at SciVerse ScienceDirect

Carbohydrate Polymers

journal homepage: www.elsevier.com/locate/carbpol

Spinning of hydroalcoholic chitosan solutions

Mylène Desorme[a,b], Alexandra Montembault[a], Jean-Michel Lucas[a], Cyrille Rochas[c], Thierry Bouet[b], Laurent David[a,*]

[a] Université de Lyon, Université Claude Bernard Lyon 1, UMR CNRS 5223, Ingénierie des Matériaux Polymères IMP@Lyon1, 15 bd Latarjet, 69622 Villeurbanne Cedex, France
[b] Laboratoire Tetra Medical, P.A.E. de Marenton, BP 142, 07104 Annonay Cedex, France
[c] Centre de Recherches sur les Macromolécules Végétales (CERMAV-CNRS, UPR 5301), Université Joseph Fourier, Boîte Postale 53, F-38041 Grenoble Cedex, France

ARTICLE INFO

Article history:
Received 21 January 2013
Received in revised form 27 March 2013
Accepted 23 April 2013
Available online 4 May 2013

Keywords:
Chitosan fiber
Hydroalcoholic chitosan solution
Physical hydrogel
Hydrophilic and hydrophobic interactions
Semicrystalline microstructure

ABSTRACT

We investigated the spinning of hydroalcoholic chitosan solutions. The dope composition was optimized in order to obtain a continuous alcogel fiber by water evaporation on heating the extruded hydroalcoholic solution. This alcogel fiber was then neutralized in aqueous alkali baths and washed in water to eliminate the residual alcohol and salts before final drying. Depending on the alcohol content in the filament at the neutralization step, on specific alcohol–chitosan interactions and on the nature and concentration of the coagulation base, the process yielded semicrystalline chitosan fibers with different proportions of anhydrous and hydrated allomorphs. Contrarily to the classical annealing method, the formation of mainly anhydrous crystals was obtained without significant molecular weight decrease by neutralizing the polymer in hydrophobic conditions. The control of allomorph content was shown to be related to the hydrophobicity of the solvent (alcohol fraction) at the neutralization step.

1. Introduction

In recent years, "new generation" medical textiles based on biomaterials with bioactive properties have received growing interest in biomedical research (Boateng, Matthews, Stevens, & Eccleston, 2008). These technologies usually involve either the incorporation of pharmaceutical or biological molecules (*e.g.* antiseptics (Meaume, Vallet, Morere, & Teot, 2005), growth factors (Puolakkainen et al., 1995)) or the use of natural polymers such as proteins (*e.g.* collagen (Parenteau-Bareil, Gauvin, & Berthod, 2010), silk fibroin (Min et al., 2004)) or polysaccharides, especially those that can express the rare property of bioactivity (*e.g.* hyaluronic acid (Chen, & Abatangelo, 1999), chitosan (Muzzarelli, 2009)). Hence, the main strategies to produce such "bioactive" fiber-based devices are: (i) the coating of conventional fibers or textiles with these biopolymers (*e.g.* Parietex®composite, Promogran®) or pharmaceutical agent (Blanchemain et al., 2008; Ravindra, Mohan, Reddy, & Raju, 2010), (ii) the incorporation of bioactive molecules into the dope to be spun (Schneider, Wang, Kaplan, Garlick, & Egles, 2009), or (iii) the direct spinning of natural bioactive polymer solutions into fibers (Agboh & Qin, 1997; Meyer, Baltzer, & Schwikal, 2010; Wang et al., 2005).

Among spinnable polysaccharides, chitosan is well-known for its biocompatibility, haemostatic, bacteriostatic and fungistatic properties, bioresorbability as well as its healing bioactivity (Domard & Domard, 2002, chap. 9), and thus constitutes an excellent candidate for smart biomedical textile applications. Indeed, chitosan fibers could be used into many product forms such as woven/non-woven dressings to limit fungal and bacterial proliferation and promote tissue regeneration (Agboh & Qin, 1997; Jayakumar, Prabaharan, Kumar, Nair, & Tamura, 2011; Muzzarelli, 2009) (*e.g.* in the case of chronic wounds); as knitted textiles to be incorporated in synthetic fiber-based textile implants to improve their biocompatibility and stimulate healing mechanisms (Burger, Halm, Wijsmuller, ten Raa, Jeekel, 2006; Earle & Romanelli, 2007); as yarns for bioresorbable surgical sutures (Ravikumar, 1999). This polysaccharide is produced from the N-deacetylation of chitin which is the most abundant polymer in biomass with cellulose (Roberts, 1992). Chitin and chitosan are linear copolymers of 2-amino-2-deoxy-β-D-glucan (GlcN) and 2-acetamido-2-deoxy-β-D-glucan (GlcNAc) residues. A key structural parameter is defined by the degree of acetylation (*DA*) corresponding to the molar fraction of GlcNAc residues. Chitosan refers to polymers soluble in dilute acid aqueous solutions at pH < 6 and thus to *DA*s below 60% for statistical copolysaccharides (Domard & Domard, 2002). The presence of only β(1→4) type glycosidic linkages along the polymer backbone (as found in the cellulose structure) yields filmogenic and fiber-forming ability useful for fiber spinning applications (Hudson,

* Corresponding author. Tel.: +33 04 72 43 16 05.
E-mail address: laurent.david@univ-lyon1.fr (L. David).

0144-8617/$ – see front matter © 2013 Elsevier Ltd. All rights reserved.
http://dx.doi.org/10.1016/j.carbpol.2013.04.070

1998; Rathke & Hudson, 1994). Thus, chitosan yarns have been mainly produced by wet-spinning (like regenerated cellulose or viscose). Other methods have been developed such as dry-jet-wet spinning (Agboh & Qin, 1997), pseudo-dry-spinning (Notin, Viton, Lucas, & Domard, 2006), later referred to as gel-spinning (Notin, Viton, David, et al., 2006), and electrospinning (Lee, Jeong, Kang, Lee, & Park, 2009; Pillai & Sharma, 2009). Except from electrospinning that is limited to the production of nanofiber mats such as non-wovens and not easily to the production of yarns, all the above techniques are based on the coagulation of aqueous chitosan solutions in alkali media. Chitosan must be dissolved in a dilute aqueous acid solution inducing the protonation of the free amino groups of glucosamine (GlcN) residues. The resulting polyelectrolyte solution is used as a spinning dope and is converted to chitosan fibers by coagulation of the polymer solution induced at pH > 6.5 (*i.e.* above the pK_0 value for chitosan with $DA < 25\%$ (Domard & Domard, 2002)) due to the regeneration of the free amino form. The alkali media is either an alkali bath (NaOH (East & Qin, 1993; Knaul & Creber, 1997) or NaOH/alcohol mixture (Molloy, 2002), KOH (El-Tahlaway & Hudson, 2006; Knaul & Creber, 1997), ammonia (Knaul & Creber, 1997)...) for wet-spinning and dry-jet-wet spinning or ammonia vapors for gel-spinning (Notin, Viton, David, et al., 2006). After washing and drying, typical tenacity can be closed to 2 g/denier in the dry state (the denier represents the mass in grams per 9000 meters of fiber). Besides their remarkable biological features, the well-known drawback of chitosan fibers is the lower mechanical properties compared with synthetic fibers. This makes difficult to perform post-operations such as weaving or knitting. Moreover, an important loss of mechanical properties is observed in wet environment (East & Qin, 1993). Improving mechanical properties both in the dry state and in contact with physiological fluids is a real challenge and brings to develop new chitosan spinning processes. Current approaches are based on chemical crosslinking (*e.g.* epichlorohydrin (Lee, Kim, & Kim, 2007; Wei, Hudson, Mayer, & Kaplan, 1992), phthalate or phosphate ions (Knaul, Hudson, & Creber, 1999a), dialdehydes such as glutaraldehyde or glyoxal (Knaul, Hudson, & Creber, 1999b; Yang, Dou, Liang, & Shen, 2005) or physical post-treatments (East & Qin, 1993; Knaul et al., 1999a; Notin, Viton, David, et al., 2006)) (*e.g.* drawing at coagulation or drying step). But the increase of mechanical properties obtained by these methods remains low (maximum tenacity of 2.4 g/denier) and other spinning routes still need to be developed to improve and control physical and biological properties of chitosan fibers.

Most of natural polymer fibers are formed from coagulated hydrogel materials (*i.e.* alginates (Qin, 2008), cellulose (Woodings & The Textile Institute, 2001), chitosan (Agboh & Qin, 1997)). The solid fibers obtained from drying a coagulated filament should inherit part of the morphology of the hydrogel (Robitzer, David, Rochas, Di Renzo, & Quignard, 2008). More precisely, the physical properties of the fibers in the dry state should depend on the polymer chain ordering resulting from intra- and intermolecular interactions in the hydrogel fiber (entanglements, hydrogen bonding, hydrophobic interactions, and electrostatic interactions if ionic complexes with the polyelectrolytes are present). Thus, the mechanical properties of final fibers should be improved by generating and preserving the maximum of polymer intra- and interchain interactions all through the fiber spinning process, from the initial solution, to the gel fiber, and in the dry fiber (Popa-Nita, Alcouffe, Rochas, David, & Domard, 2010).

Thus, physical chitosan hydrogels with a relatively high mechanical strength can be obtained by neutralizing concentrated aqueous chitosan solutions of high molecular mass in alkali baths (Araiza, Rochas, David, & Domard, 2008) or in ammonia vapors (Montembault, Viton, & Domard, 2005a). Indeed, most chitosan spinning techniques are based on these gelation methods (Agboh & Qin, 1997; Notin, Viton, David, et al., 2006; Rathke & Hudson, 1994; Ravikumar, 1999). A second route to obtained physical chitosan hydrogels is the neutralization in alkali baths of alcoholic chitosan gels (that will hereafter be referred to as alcogels) produced hydroalcoholic chitosan solutions by water evaporation (Montembault, Viton, & Domard, 2005b). In that case, the mechanical properties of chitosan hydrogels are significantly improved compared with the aqueous process, suggesting a higher density of chain entanglements and junctions inherited from the alcogel (Montembault et al., 2005b; Montembault, Viton, & Domard, 2005c). Therefore, in the present work, we investigated the spinning of hydroalcoholic chitosan solutions. The gelation of the extruded solution was induced by selective solvent evaporation (water evaporation) at moderate temperature ($T \sim 130\,^{\circ}C$) to form an alcoholic chitosan gel fiber. This alcogel fiber was then neutralized in an alkali bath to obtain a stable physical hydrogel. After washings in water and drying, the process led to a pure chitosan fiber. In this work, the chitosan dope composition (*i.e.* polymer concentration, water/alcohol ratio in the initial solvent, alcohol nature and chitosan salt form), the post-extrusion thermal treatment, as well as the neutralization conditions (*i.e.* base nature and concentration) were studied and optimized for spinning. In addition, thanks to X-ray diffraction techniques, we studied the influence of all these physico-chemical parameters on the final semi-crystalline microstructure of chitosan fibers. We evidenced different semi-crystalline morphologies that provide new perspectives in controlling the morphology, and thus the physical and biological properties of chitosan fibers.

2. Materials and methods

2.1. Materials

A weakly acetylated chitosan with a high molecular weight produced from squid pens was supplied by Mahtani Chitosan Pvt. Ltd. (batch type 113, dated 17/12/2004) and characterized as previously described (Boucard, Viton, & Domard, 2005; Montembault et al., 2005b) (Table 1). All the polyols (purity of 99%) used to prepare hydroalcoholic chitosan solutions as well as concentrated ammonium hydroxide solution and sodium hydroxide pellets were purchased from Acros organics or Sigma Aldrich.

2.2. Preparation of hydroalcoholic chitosan dopes and rheological measurements

2.2.1. Preparation

Chitosan was dispersed in deionized water. Acetic acid (or hydrochloric acid in some experiments) was added to achieve the stoichiometric protonation of free amine sites of D-glucosamine residues. Stoichiometric protonation conditions (*i.e.* no acid excess) were chosen in order to avoid the polymer degradation and the neutralization kinetics decrease (El-Tahlaway & Hudson, 2006). Alcohol (*e.g.* 1,2-propanediol) was added slowly (3 additions over 2 h) only after complete dissolution of chitosan in aqueous media and the blend was stirred for 5 h to complete homogenization. In all hydroalcoholic chitosan solutions, the polymer concentration is largely over the critical chain entanglement concentration ($C^* = 1/[\eta]$) = 0.06–0.1% (w/w) (Boucard et al., 2005; Montembault et al., 2005b). Different water/alcohol (w/w) ratios were tested. Thus, in the initial aqueous solution, the chitosan concentration was adjusted depending on the targeted water/alcohol ratio and the polymer concentration required in the final solution.

2.2.2. Rheological measurements

Rheological measurements were conducted on a stress-controlled rheometer (AR 2000, TA Instruments) at $22 \pm 2\,^{\circ}C$. The steady viscosity of chitosan solutions was assessed in static mode

Table 1
Physico-chemical characterization of the chitosan used in this work: degree of acetylation (*DA*) from ^{1}H NMR, weight-average molecular weight (M_w), weight-average degree of polymerization (DP_w) and polydispersity index (I_p) from SEC coupled with multi-angle light scattering and refraction index measurements, and water content from thermogravimetric analysis.

DA (%)	M_w (g/mol)	DP_w	I_p	Water content (%)
1.5 ± 0.2	410,000 ± 40,000	2600 ± 260	1.6 ± 0.3	9.8 ± 1.0

using aluminum cone-plate geometry (25 mm diameter; 4°) to ensure a uniform shear rate. The minimum gap was fixed at 114 μm. All measurements were carried out at applying successive shear rates ranging from 1.25×10^{-3} to 10 s^{-1} and repeated two times. The linear viscoelastic behavior of some chitosan solutions in dynamic mode was also investigated. A 25-mm parallel plate geometry was used in this case with a 500 μm gap. For each measurement, the conditions of linear viscoelastic regime were first determined by performing a stress sweep test at a constant angular frequency of 10 rad s^{-1}. The applied shear stress to remain in the viscoelastic regime was chosen as 100 Pa for all samples. Angular frequency sweep measurements were then performed in the range from 100 rad s^{-1} down to 10^{-1} rad s^{-1}. Silicon oil was spread onto the external surfaces of the samples to prevent evaporation during the experiment.

2.3. Chitosan fiber preparation

The hydroalcoholic chitosan dopes were prepared as described in Section 2.2 and degassed by centrifugation at 10,000 rpm for 5 min. This degassing method was efficient compared with other vacuum methods and ensured a constant dope composition. The extrusion step was performed at laboratory scale by means of a metering pump (from 0.8 to 40 mL/h), a polypropylene syringe (V = 10 mL) and a stainless steel needle as a spinneret (Sterican® B-Braun non-beveled needle tip having a 800 μm internal diameter and a 22 mm length). The dope was extruded at a rate of 12.7 mL/h and the gelation was induced by subjecting the extruded solution for about 20 s to a hot air flow at 130 °C produced by a heat gun (length of air flow chamber: 30 cm). The temperature at the end of the spinneret was checked to be at 130 ± 5 °C in all experiments. In all spinning runs, the extrusion rate was maintained at 0.2 mL/min corresponding to the minimum extrusion rate value that prevented the alcogel formation within the spinneret. The alcogel monofilaments were then neutralized in alkali media (aqueous NaOH or NH_4OH solutions at 1, 4 and 10 M) to fully regenerate the free amine form of chitosan and avoid any re-dissolution of filaments in water ($t_{neutralization}$ = 1 min, V_{bath} = 250 mL). Then, the neutralized fibers were successively immersed in 3 washing baths containing deionized water to fully eliminate the excess of base, the alcohol and the salts generated during neutralization ($t_{washing}$ = 3× 10 min, V_{bath} = 250 mL). Finally, the chitosan fibers were dried overnight at 40 °C at constant length. The fiber diameter after extrusion is closed to the spinneret diameter (~800 μm). After drying, the diameter is reduced to 60–80 μm depending on fiber stretching.

2.4. Chitosan fiber characterization

2.4.1. Wide angle X-ray scattering (WAXS)

Wide-angle X-ray scattering was performed on the BM2-D2AM beamline at the European Synchrotron Radiation Facility (Grenoble, France). The data were collected at an incident photon energy of 16.000 keV (λ = 0.775 Å) using a bi-dimensional detector (CCD camera from Ropper Scientific) positioned at 6–14 cm from the sample, depending on synchrotron experiment runs. Exposure time was set at 20 s. Chitosan fibers were wrapped around brass sample holder plates with a 6 mm hole in the center. Four V-shaped lateral notches on holder plates allowed to wrap the fibers with a 8-shaped path to allow the irradiation of only one bundle of fibers in the hole (Fig. 1).

Wrapped samples were placed on a multi-sample holder so that the fiber axis is horizontal and perpendicular to the incident beam. Silver behenate, zinc oxide (blende) and quartz (alpha) were used as standards for the scattering vector (q-range) calibration. Primary data corrections, *i.e.* dark current, flat field response and taper distortion were performed thanks to the bm2img software available on the beamline. The scattered intensity of the samples was automatically normalized by the transmitted intensity. Additional corrections for the background scattering (subtraction of the empty cell) and the sample effective thickness were performed for each pattern. 2D images were converted into radial averages over the image center (position of the center of the incident beam) to give the scattered intensity I *vs* the scattering vector q. Since an anisotropic scattering was observed with the fiber samples, the scattering intensity was also recorded as a function of the azimuthal angle φ (48 sectors with 7.5° width to give $I(q, \varphi) = f(q, \varphi)$ profiles). In our experiments, as the fiber samples were placed horizontally, φ = 0 and 180° on the horizontal direction (parallel to the fiber axis) and φ = 90 and −90° on the vertical direction (perpendicular to the fiber axis).

Diffraction patterns obtained from radial averages were used to evaluate the overall crystallinity index (*CI*) of chitosan fibers given by the following relation (Osorio-Madrazo et al., 2010):

$$CI = \frac{A_c}{A_c + A_a} \quad (1)$$

where A_c and A_a are the sum of areas under the crystalline and amorphous peaks, respectively. Contrary to other methods based on the estimation of a diffuse amorphous background (Abdou, Nagy, & Elsabee, 2008; Focher, Beltrame, Naggi, & Torri, 1990; Toffey & Glasser, 1999), we chose to determine the amorphous contribution from the diffractogram of an amorphous sample of chitosan (Osorio-Madrazo et al., 2010) (see details in Section 3.4.1). To obtain such a sample, chitosan was dispersed at C_p = 2% (w/w) in dilute acid aqueous solution containing the stoichiometric amount of acetic acid necessary for the $-NH_2$ sites protonation. After the complete polymer dissolution, 3 g of solution were placed in a Petri Dish (2 cm diameter) and left to evaporate overnight in an oven at 50 °C to lead to the formation of an amorphous film.

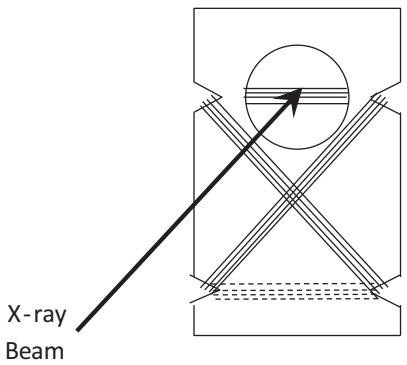

Fig. 1. Schematic representation of chitosan fibers wrapped around the 4 V sample holder plate (2 cm × 1 cm).

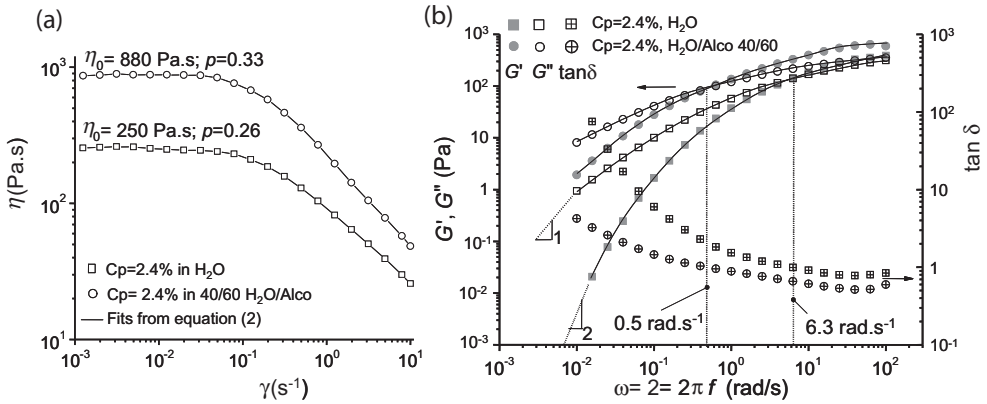

Fig. 2. Influence of the solvent nature on the rheological behavior of chitosan acetate solutions at 22 °C (C_p = 2.4 wt%, DA ~ 1.5%, M_w ~ 410,000 g/mol): (○) 40/60 (w/w) water/1,2-propanediol solvent mixture and (□) water; (a) variation of steady viscosity η *vs* shear rate $\dot{\gamma}$ (experimental data and fits determined from the Carreau model (Eq. (2)); (b) storage (G') and loss (G'') shear moduli and tan δ as a function of frequency of two different solutions.

From the $I(q, \varphi)$ profiles, we extracted the average scattered intensity at φ = 90 and −90° (average on vertical sectors centered at [82.5°; 97.5°] and [−82.5°; −97.5°]), for which the maximum scattering intensities were observed due to the preferential orientation of the chain axis of the crystallites along the fiber axis. These intensity profiles recorded perpendicular to the fiber axis were used as a comparative tool to assess the evolution of the allomorph composition in the chitosan fibers as a function of the chitosan dope composition and the coagulation conditions. The proportion in anhydrous and hydrated allomorph in chitosan fiber samples was estimated semi-quantitatively after subtraction of the amorphous background.

3. Results and discussion

3.1. Conditions for alcogel formation and spinning ability ("spinnability")

We determined the physico-chemical parameters suitable for the alcogel fiber formation to develop an alcogel-spinning process, on the basis of several previous works (Boucard et al., 2005, 2007; Montembault et al., 2005b). In contrast with the discontinuous elaboration of cylindrical hydrogels, we deal with a continuous process in a spinning approach. In this case, the gelation kinetics must be fast, and optimized in order to obtain a continuous alcogel filament (*i.e.* highly enriched in alcohol) without disruption at the end of the spinneret. In previous works (Boucard et al., 2005; Montembault et al., 2005b), several physico-chemical parameters were evidenced to influence on the alcogel gelation kinetics of hydroalcoholic chitosan solutions: (i) the degree of acetylation (DA), (ii) the polymer concentration (C_p), (iii) the acid used for chitosan dissolution, (iv) the 1,2-propanediol proportion in the initial solvent, (v) the temperature used to induce solvent evaporation and (vi) the surface/volume ratio for drying. In this work, considering the final applications of chitosan fibers as biomedical textiles, we decided to use a low DA (~1.5%) associated with a high molecular weight (~410,000 g/mol) to limit the fiber redissolution at physiological pH (Vårum, Ottøy, & Smidsrød, 1994) and favor good mechanical properties (Agboh & Qin, 1997). Moreover, the regularity of the macromolecular structure, which usually helps the development of crystallinity (Peters, 1963), is increased for low DA, N-acetyl-glucosamine residues can be considered as crystalline defects. Concerning biological properties, low DA and high molecular weight chitosans showed higher bioresorption times (Tomihata & Ikada, 1997), property that would be valorized for textile implant applications. In order to increase the gelation kinetics and avoid the filament breakage at the end of the spinneret, high evaporation temperatures (Montembault et al., 2005b) (T ~ 130 °C), high 1,2-propanediol contents (above 60% (w/w), see below) in the initial hydroalcoholic chitosan dope, as well as high polymer concentrations (above 2%, w/w) must be favored (Boucard et al., 2005; Montembault et al., 2005b). The spinnability of the hydro-alcoholic polymer solution will thus be defined in this work as the ability to form a continuous and stable alcogel filament from the end of the spinneret to the end of the heating chamber (hot air gap of 30 cm), without breakage of the thread line in the part close to the spinneret end during the sol/alcogel transition. The temperature of the hot air chamber was constant at 130 °C to significantly increase the gelation kinetics (Montembault et al., 2005b) without inducing a thermal degradation of chitosan (Osman, 2005). Spinnability depends on many variables (Ziabicki, 1976) acting on the gelation kinetics, but is also related to the rheological properties of the dope (McKinley, 2005). The rheological behavior of chitosan dopes is in turn mainly governed by the polymer concentration, the polymer molecular weight, the solvent nature and composition used for the polymer dissolution.

3.2. Effect of the addition of alcohol on viscoelastic properties of chitosan solutions

The typical flow curves of hydroalcoholic and aqueous chitosan solutions are shown in Fig. 2a. The well-known shear thinning behavior of chitosan solutions (Calero, Munoz, Ramirez, & Guerrero, 2010; Desbrieres, 2002) was observed in both media. It is characterized by a critical shear rate above which the viscosity decreases. This effect has been attributed to polymer chain disentanglements and/or interchain junction breakdown under shear (Merkovich et al., 2001). The viscosity was analyzed in the entire shear rate range using the three-parameter Carreau model (Cho, Heuzey, Begin, & Carreau, 2006) in order to deduce the Newtonian viscosity η_0 from the extrapolation of the viscosity at zero shear rate:

$$\eta = \frac{\eta_0}{(1 + (\tau_R \dot{\gamma})^2)^p} \quad (2)$$

where τ_R is the relaxation time for chain disentanglement and p is a shape coefficient.

As illustrated in Fig. 2a, a significantly higher viscosity was obtained in the case of the mixed water/1,2-propanediol solvent medium compared with the aqueous solution for an equivalent polymer concentration in the solution (C_p = 2.4% (w/w)). The comparison of linear viscoelastic properties of hydroalcoholic and aqueous chitosan solutions was also investigated thanks to

oscillatory shear measurements. Fig. 2b displays the evolution of the storage (G') and loss (G'') moduli as well as the loss tangent ($\tan\delta$) as a function of the angular frequency. Both solutions exhibited a rheological behavior typical of viscoelastic solutions with $G' < G''$ at low frequency and $G' > G''$ at high frequencies. Again, this crossover between G' and G'' is commonly reported in the case of concentrated high molecular weight chitosan solutions and has been associated to the phenomenon of chain disentanglements and interchain junction breakdown (Calero et al., 2010; Serrero et al., 2010). The characteristic slopes $G'' \sim \omega^1$ and $G' \sim \omega^2$ at low frequencies described for viscoelastic fluids in the Maxwell model were compatible with the behavior of the chitosan aqueous solutions only in the low frequency limit. At constant $C_p = 2.4\%$ (w/w), the presence of 1,2-propanediol in the solvent (*i.e.* 40/60 (w/w) H_2O/alcohol ratio) resulted in an increase in both G' and G'' in agreement with the solution viscosity increase observed in flow regime. Furthermore, the cross-over angular frequency where $G' \sim G''$ (see Fig. 2b), which is related to a characteristic life time of interchain interactions ($\lambda_0 = 1/\omega_c$), occurred at lower frequency compared to the aqueous system (*i.e.* 0.5 *vs* 6.3 rad s^{-1}). Thus, in the hydroalcoholic medium, the time for chitosan chain disentanglement and interchain junction breakdown is significantly higher (factor 12) reflecting a higher entanglement density or the formation of a higher number of interchain junctions in the presence of 1,2-propanediol. This effect was also confirmed by the smaller value of $\tan\delta$ in the case of the hydroalcoholic solution in the investigated frequency range as well as a lower slope in the high frequency side of the Cole–Cole diagram (Fig. 3), characteristic of a larger number of interchain junctions. The Cole–Cole plots were further analyzed with Havrilia–Negami equation (Havrilia & Negami, 1967):

$$\frac{\eta}{\eta_0} = \frac{1}{(1 + (i\omega\tau)^{\alpha})^{\beta}} \quad (3)$$

where the exponent product $\alpha \cdot \beta$ is related to the breadth of the relaxation time distribution and parameter β is an asymmetric distribution parameter.

Both water and water/alcohol systems exhibit a distribution of relaxation times since α and $\beta < 1$. The presence of alcohol in the dope results in a more symmetric but broader relaxation time distribution ($\alpha \cdot \beta$ decreases and β increases in the presence of alcohol). As a conclusion, the addition of alcohol molecules in the solvent favors chitosan chain entanglements and interchain interactions. A linear increase of the Newtonian viscosity of the dope was observed with the increase of the 1,2-propanediol proportion in the initial

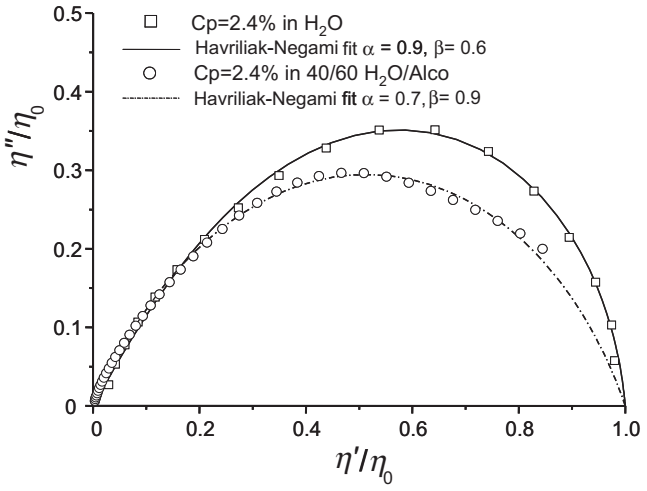

Fig. 3. Normalized Cole–Cole diagram of chitosan acetate solutions at 22 °C ($C_p = 2.4$ wt%, $DA \sim 1.5\%$, $M_w \sim 410{,}000$ g/mol) (○) in 40/60 (w/w) water/1,2-propanediol solvent mixture and (□) in water.

solvent for $C_p = 2.4\%$ (w/w) (Fig. 4a). This effect must be related to the progressive decrease of the solvent dielectric constant induced by the increase of the alcohol content in the solvent. In hydroalcoholic medium, the dissociation of acetic acid is disfavored. The resulting decrease of the apparent charge density of chitosan in presence of alcohol was established by Boucard et al. (2007). In this context, the electrostatic repulsions between chitosan chains should be reduced in favor of the formation of interchain hydrogen bonding and hydrophobic interactions. In addition, the formation of junctions between chitosan chains could be reinforced by the presence of the alcohol molecules themselves: the diol could act as a bridging agent by the establishment of hydrogen bonds with the polymer (Quijada-Garrido, Iglesias-Gonzalez, Mazon-Arechederra, & Barrales-Rienda, 2007). Such interactions have been invoked by Boucard (Boucard et al., 2005) and Montembault (Montembault et al., 2005b) to explain the formation of alcoholic chitosan gels. The increase of entanglement density and chitosan chain interchain interactions in hydroalcoholic medium is a key feature to increase polymer chain junctions into the dope and improve the mechanical properties of the resulting fibers in comparison with the processing of aqueous chitosan dopes.

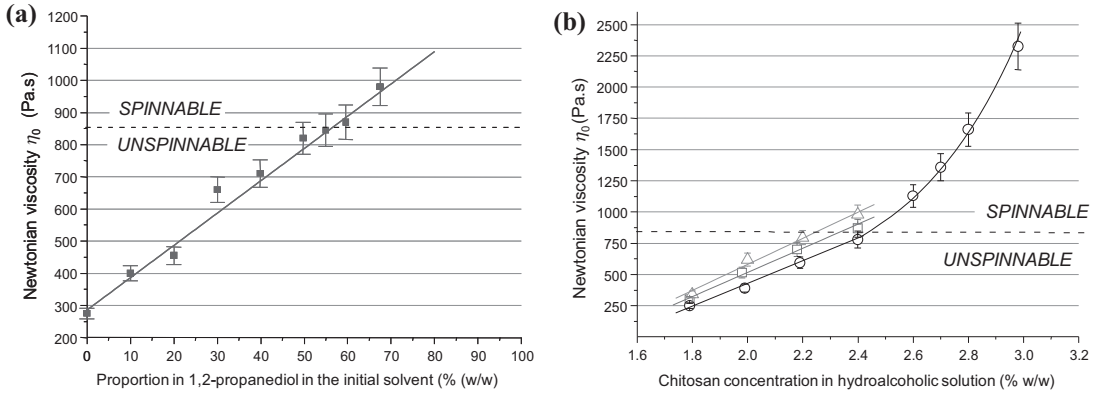

Fig. 4. Influence of the water/1,2-propanediol ratio and the chitosan concentration on the hydroalcoholic dope viscosity and spinnability. (a) Viscosity at 22 °C of a 2.4% (w/w) hydroalcoholic chitosan solution in different water/1,2-propanediol mixtures for $C_p = 2.4\%$ (w/w). (b) Viscosity at 22 °C of hydroalcoholic chitosan solutions as a function of polymer concentration for 3 different water/1,2-propanediol ratios: (○) 50/50 (w/w), (□) 40/60 (w/w) and (△) 30/70 (w/w). The dotted line represents the limit between the spinnable and unspinnable domains ($\eta_0 \sim 850$ Pa s) for a chitosan with $DA \sim 1.5\%$, $M_w \sim 410{,}000$ g/mol.

Table 2
Chitosan concentrations ($C_p \pm 0.1\%$ (w/w)) achievable in final hydroalcoholic solutions with various water/1,2-propanediol ratios from initial aqueous polymer solutions of different concentrations. Newtonian viscosity values η_0 (±8%) were indicated for initial aqueous chitosan solutions.

Initial aqueous chitosan solution		C_p (%, w/w) in final hydroalcoholic solution for various water/alcohol (w/w) ratios		
C_p (%, w/w)	η_0 (Pa s)	50/50	40/60	30/70
4%	10,800	2%	1.6%	1.2%
6%	45,000	3.1%	2.5%	1.9%
8%	>60,000	4.2%	3.4%	2.6%

3.3. Optimization of the hydroalcoholic chitosan dope composition for spinnability

3.3.1. Influence of polymer concentration and water/1,2-propanediol ratio

The composition range of the hydroalcoholic dopes (polymer concentration and alcohol content) that can be explored for spinnability was limited for practical reasons. Indeed, the complete dissolution of chitosan can only be achieved in aqueous acid medium. In a second step, hydroalcoholic chitosan solutions are prepared by addition of alcohol to the aqueous solution. Due to the polyelectrolyte nature of chitosan in aqueous acid solutions, the viscosity of chitosan solutions drastically increases with polymer concentration (Martinez, Chornet, & Rodrigue, 2004; Mucha, 1997). Above $C_p = 6\%$ ($DA \sim 1.5\%$ and $M_w \sim 410{,}000$ g/mol), homogeneous aqueous chitosan solutions are difficult to obtain as Newtonian viscosities exceed 45,000 Pa s. In these conditions, the maximum polymer concentration in the hydroalcoholic dope was 3.1%, 2.5% and 1.9% (w/w) for 50/50, 40/60 and 30/70 (w/w) water/1,2-propanediol mixtures, respectively (Table 2).

The evolution of the solution viscosity as a function of the alcohol content in the initial solvent mixture is represented in Fig. 4a for a constant chitosan concentration $C_p = 2.4\%$ (w/w). Fig. 4b displays the evolution of the hydroalcoholic dope viscosity with the polymer concentration at a given water/alcohol ratios (50/50; 40/60; and 30/70 (w/w)). The combined effect of the polymer concentration and the water/1,2-propanediol ratio on spinnability of chitosan dopes ("alco-gelability") was examined to define the spinnability range. As expected, the gelation of the liquid thread line was favored on increasing the 1,2-propanediol proportion in the initial solvent (Fig. 4a) and on increasing the polymer concentration (Fig. 4b) due to a higher density of chain entanglements/interactions in the initial dope inducing a faster establishment of the physical network. Accordingly, the spinnability of the hydroalcoholic dope was obtained above a critical viscosity located around 850 Pa s. Nethertheless, the use of a polymer concentration above 2.8% in the hydroalcoholic solution drastically increased the degassing time and also the pressure needed to ensure the correct charge of the pump at a given flow rate. In our experimental conditions with chitosans of high molecular mass, satisfactory spinning conditions were found at a chitosan concentration of 2.4% in a mixture 40/60 (w/w) water/1,2-propanediol (Fig. 5).

3.3.2. Influence of alcohol structure

The formation of alcoholic chitosan gels could be achieved with other alcohols than 1,2-propanediol. As reported in a previous work (Boucard et al., 2005), the nature of the alcohol has an influence on both the gelation process and the physical properties of the resulting alcogels. Therefore, the spinnability of chitosan hydroalcoholic dopes and the physical properties of the fibers could be improved depending on the alcohol used to induce the polymer gelation. We tested different polyhydroxylated alcohols with short alkyl lengths (3–4 carbons) and high boiling point temperatures ($b.p. > 180\,^{\circ}C$).

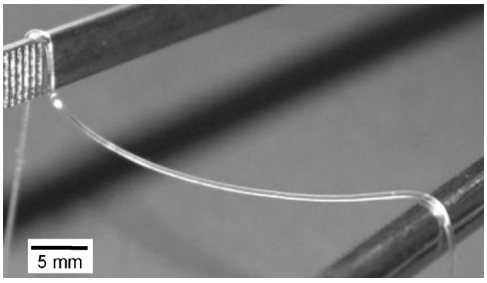

Fig. 5. Alcogel chitosan filament obtained from the gelation at 130 °C of a 2.4% (w/w) polymer solution in a 40/60 (w/w) water/1,2-propanediol mixture.

These parameters were identified by Boucard et al. (2005) as the critical criterions to obtain the alcogel formation since no macroscopic gelation occurred with monoalcohols or polyols of higher alkyl chain length (5 carbons and more). Besides the alkyl chain length, the alcohols tested for spinning differed by the position and the number of hydroxyl functions. To compare the different dopes, we used the optimum composition determined previously, *i.e.* $C_p = 2.4\%$ (w/w) and water/alcohol ratio = 40/60 (w/w). The viscosity of each dope and its ability to form an alcogel filament in the 130 °C air drying chamber ($t_{130\,^{\circ}C} \sim 20$ s) are summarized in Table 3.

The viscosity of the dope was shown to be strongly influenced by the nature of the alcohol with no direct relation with the dielectric constant or the viscosity of pure alcohols. The viscosity differences may thus arise from specific interactions between alcohol molecules and chitosan chains depending on the chemical structure of the alcohol. Indeed, when comparing the results obtained with the three different propyl chain length alcohols (*i.e.* 1,2- and 1,3-propanediol and glycerol), we noticed that both the position and number of hydroxyl groups impacted the final dope viscosity. In addition, for alcohols with similar positions hydroxyl groups (*e.g.* 1.3-propanediol and 1,4-butanediol), the alkyl chain length also appeared to have a significant effect on viscosity. An important evolution of dope viscosity was also observed with the storage time in the case of 1,3-propanediol. The dope viscosity drastically increased from 1500 Pa s to 2700 Pa s after one day of storage in a closed reactor at ambient temperature and the solution spontaneously turned to a gel after several days without observing any solvent loss from the dope. For all the polyols tested in this work, we obtained the formation of a continuous alcogel filament after extrusion in the 130 °C air drying chamber ($t_{130\,^{\circ}C} \sim 20$ s). However, the use of glycerol in the spinning dope did not lead to a homogeneous gel filament at a water/alcohol ratio of 40/60 (w/w). A heterogeneous syneresis occurred as glycerol was expelled from the polymer network along the filament (results not shown). This phenomenon could be the result of strong chitosan–glycerol interactions. In our experimental conditions, spinning runs with 1,3-propanediol and butyl chain length diols led to alcogel filaments with improved mechanical strength compared with 1,2-propanediol. These observations may result from the higher initial dope viscosities measured for these alcohols suggesting stronger alcohol–chitosan chain interactions. In these conditions, the gel point could be reached faster resulting in increased mechanical properties of alcogel fibers. At last, the use of a mixture of alcohols could be possible to modulate the dope viscosity but was not considered in this work.

3.3.3. Influence of counter-ion nature

The formation of alcoholic chitosan gels is not limited to the acetate form of chitosan and can also be obtained with the hydrochloride form (Boucard et al., 2005). We studied the influence of the two counterion forms on the formation of the alcogel filament. Again, the optimum composition determined for acetate chitosan (*i.e.* 2.4% of polymer in 40/60 1,2-propanediol/water

Table 3
Chemical structure and physical constants (Lide, 2010) of the different polyols tested and their influence on the viscosity and spinnability of corresponding hydroalcoholic dopes (C_p = 2.4% (w/w) and 40/60 (w/w) water/alcohol ratio).

Alcohol	Chemical structure	*b.p.* (°C)	*d*	Dielectric constant	Alcohol Viscosity at 20 °C (Pa s)	Chitosan dope viscosity (Pa s)	Observations
1,2-Propanediol	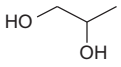	187	1.03 (20 °C)	32 (22 °C)	1.4324	890 ± 70	Stable alcogel fiber
1,3-Propanediol		215	1.053 (20 °C)	35 (22 °C)	1.4398	1500 ± 120	Very stable alcogel fiber formation but instability of the dope viscosity which drastically increased with storage time
1,2-Butanediol	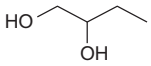	192	1.006 (25 °C)	30 (17 °C)	1.4375	1060 ± 90	Very stable alcogel fiber
1,3-Butanediol	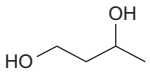	204	1.004 (20 °C)	28.8 (25 °C)	1.4418	1350 ± 110	Very stable alcogel fiber
1,4-Butanediol	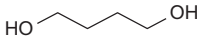	235	0.988 (20 °C)	31.4 (25 °C)	1.446	1250 ± 100	Very stable alcogel fiber
Glycerol	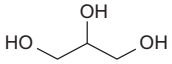	290	1.26 (20 °C)	42.5 (20 °C)	1.4746	1950 ± 160	Alcogel fiber formation but observation of syneresis phenomenon

mixture) was chosen for the comparison of the spinning runs. Despite the slightly higher dope viscosity observed in the case of hydrochloride chitosan (1020 ± 80 Pa s *vs* 890 ± 70 Pa s for the acetate form at same pH 5), frequent disruptions of the fluid thread line occurred in the immediate vicinity of the spinneret under the own weight of the filament. Therefore, hydroalcoholic solutions of chitosan hydrochloride could not lead to the formation of an alcogel fiber. This result should arise from the slower gelation kinetics of chitosan in hydroalcoholic medium in the case of the hydrochloride salt form (Boucard et al., 2005). Contrary to hydrochloride acid, a part of acetic acid can be evaporated from the solution during the thermal treatment at 130 °C and can thus induce a beginning of polymer neutralization (Demargerandre & Domard, 1994) favoring the gelation process in alcoholic media.

3.4. Crystalline microstructure of chitosan fibers

In the global frame of polymeric fiber development, microstructural parameters (Ibanes et al., 2004) such as molecular orientation, micro/nano fibrillar and semi crystalline morphology (crystallinity index, allomorph type) and intra/inter fibrillar interactions are keys for final properties and need to be closely related to processing parameters. In particular, crystallites can act as physical fillers and crosslinks of high functionality. Two allomorphs, *i.e.* hydrated ("tendon") and anhydrous ("annealed"), are described for chitosan in the free amine form (Okuyama, Noguchi, Miyazawa, Yui, & Ogawa, 1997; Yui et al., 1994). Due to the strong affinity of the polymer with water, the hydrated form, characterized by the presence of water molecules within the unit cell, is the usual allomorph obtained from the heterogeneous deacetylation of semicrystalline chitin. In the anhydrous form, the unit cell is free of water and is thus more compact. Anhydrous crystallites could then lead to a better reinforcement effect, and/or induce different biological properties.

In this work, as chitosan is dissolved in acid solution before extrusion, the native crystalline organization of chitosan is fully lost and the microstructure in final chitosan fibers will only depend on the processing parameters (*e.g.* neutralization conditions; spinning dope composition; post-extrusion thermal treatment). The wide-angle X-ray scattering (WAXS) of synchrotron radiation was used for the microstructural characterization of chitosan fibers produced from hydroalcoholic dopes in various physico-chemical contexts.

3.4.1. Influence of neutralization conditions

The effect of the neutralization conditions on the final semicrystalline structure was studied on chitosan fibers produced from our standard spinning dope (*i.e.* 2.4% (w/w) of chitosan acetate in a 40/60 (w/w) water/1,2-propanediol mixture). The post-extrusion thermal treatment was set at 130 °C during 20 s. The diffraction peaks of chitosan in alcogel and hydrogel fibers (*i.e.* obtained after neutralization of alcogel fibers and washings in water) were not clearly observed, due to the presence of a dominant scattering of alcohol or water and the low crystallinity of samples. All diffraction experiments were thus performed on final dried fibers. Fig. 6 displays the 2D-WAXS patterns of both non-neutralized dried alcogel fibers (Fig. 6a) and dried hydrogel fibers neutralized in ammonium hydroxide or sodium hydroxide at different concentrations (Fig. 6b). An anisotropic scattering is observed in all cases but the non-neutralized alcogel fiber pattern revealed a significantly weaker scattered intensity compared with neutralized samples. Thus, the development of crystallinity mainly occurs during the polymer neutralization and the crystallites are preferentially oriented with chain direction along the fiber axis. We also observed the formation of the different crystalline morphologies, *i.e.* the formation of the two allomorphs in different proportions, depending on the neutralization conditions. In the case of ammonium hydroxide neutralization, in the concentration range from 1 M to 10 M, we observed the diffraction pattern specific to the anhydrous form of chitosan. The conversion of the 2D-diffraction patterns into the average scattering intensity at $\varphi = 90$ °C and $\varphi = -90$ °C as a function of the scattering vector q (Fig. 7) confirmed the presence of the anhydrous allomorph: a diffraction peak at $q \sim 1.077$ Å^{-1} corresponding to the $(1\,1\,0)_{an}$ reflection, and a multiple peak around 1.45 Å^{-1} mainly corresponding to the $(0\,1\,2)$ and $(0\,2\,0)_{an}$ planes at $q \sim 1.413$ Å^{-1} and 1.478 Å^{-1}, respectively. In the case of sodium hydroxide neutralization, a transition of allomorph composition

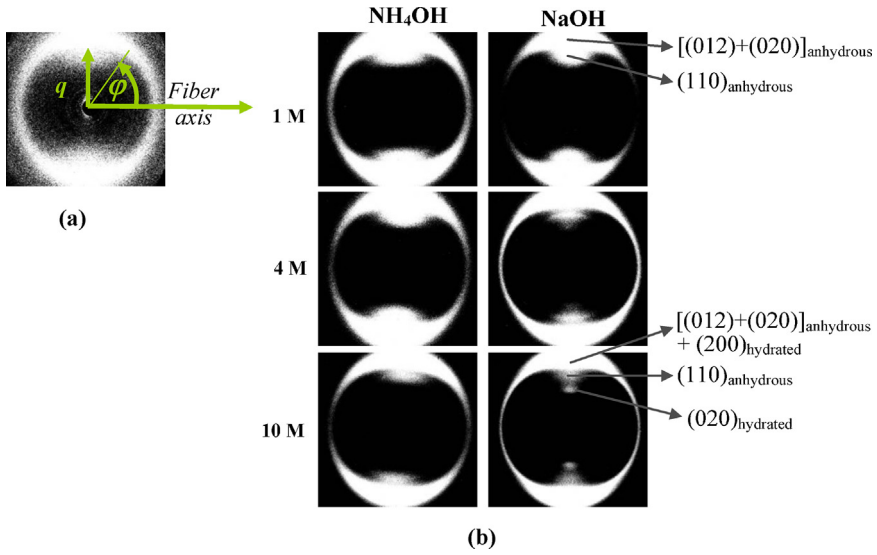

Fig. 6. Wide-angle X-ray scattering patterns (WAXS) of (a) non-neutralized chitosan alcogel fibers obtained after successive evaporations of 20 s at 130 °C and one night at 40 °C and (b) final chitosan fibers obtained by neutralization of alcogel fibers in NaOH and NH_4OH aqueous solutions at different concentrations. The initial composition of the dope was 2.4% (w/w) of chitosan in a mixture water/1,2-propanediol 40/60 (w/w).

occurred on increasing the base concentration. While the formation of the anhydrous allomorph is observed for C_{NaOH} = 1 M, the occurrence of a third spot on the diffraction patterns obtained for higher concentrations in NaOH (4 M and 10 M) revealed the formation of a mixed morphology with the presence of both anhydrous and hydrated allomorphs of chitosan (Fig. 6). The intensity of the diffraction spot located at $q \sim 0.744$ Å corresponding to $(0\,2\,0)_h$ reticular planes of the hydrated form was particularly well defined for C_{NaOH} = 10 M. At this concentration, the diffraction pattern was dominated by the presence of the hydrated form, whereas at the intermediate concentration of 4 M, the predominant crystalline phase was still the anhydrous allomorph (Fig. 7). The breadth of diffraction peaks suggested the formation of rather small or defective crystallites in both allomorph forms. The deconvolution of such diffraction patterns (Binias, Boryniec, & Binias, 2005) into a hydrated, anhydrous and amorphous contribution with Gaussian or Lorentzian peaks was difficult. Indeed, it seemed that a broad intermediary contribution between 0.74 $Å^{-1}$ and 1.077 $Å^{-1}$ could correspond to crystals that are partially anhydrous and hydrated. As a consequence, the areas under the diffraction peaks could not be clearly separated. We thus defined an anhydrous index calculated from the scattered intensity values at the expected scattering vectors of the main reflections of each allomorph according to the following relation:

$$\text{Anhydrous index} = \text{AI} = \frac{I_{anhydrous(q=1.077\,Å^{-1})}}{I_{hydrated(q=0.74\,Å^{-1})} + I_{anhydrous(q=1.077\,Å^{-1})}} \times 100 \quad (4)$$

The contribution of the amorphous background was beforehand subtracted from all chitosan fiber samples based on the same method as used for previous crystallinity index determinations (Osorio-Madrazo et al., 2010) (see below). The amorphous halo was adjusted to the diffractograms of the fiber samples at $q \sim 1.75$ $Å^{-1}$ (see Fig. 8). The results are shown in Table 4. The anhydrous index (*AI*) values reflect the evolution of the allomorph composition although they cannot be interpreted as a true atomic or weight fraction of each allomorph. In accordance with previous qualitative observations (see Fig. 7), the *AI* stayed constant whatever the base concentration in the case of neutralization in NH_4OH; whereas for NaOH neutralization, the anhydrous index decreased on increasing the base concentration. Therefore, the alcogel-spinning of hydroalcoholic solutions led to the formation of semi-crystalline chitosan fibers containing from mainly

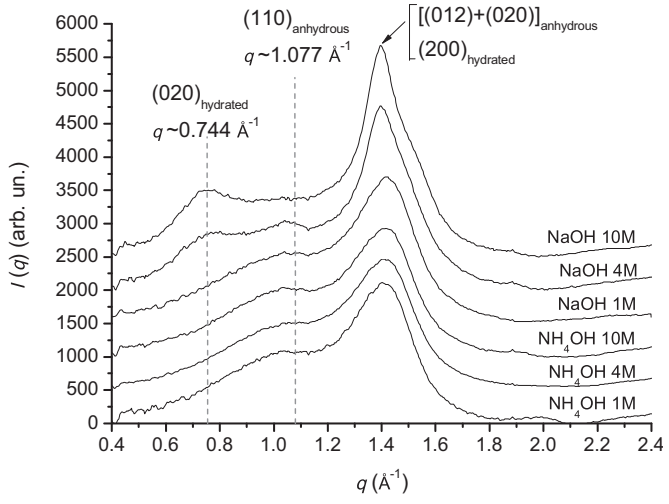

Fig. 7. Influence of neutralization conditions on the allomorph formation in chitosan fibers (initial dope composition: 2.4% of chitosan in a 40/60 (w/w) water/1,2-propanediol mixture; post-extrusion thermal treatment: 20 s at 130 °C followed by one night at 40 °C). Average WAXS patterns at $\varphi = 90°$ and $\varphi = -90$ °C after subtraction of the amorphous contribution. Scattering curves were 500 arbitrary unit vertically shifted for improved clarity.

Table 4
Values of anhydrous allomorph Index in obtained chitosan fibers (initial dope composition: 2.4% of chitosan in a 40/60 (w/w) water/1,2-propanediol mixture; post-extrusion thermal treatment: 20 s at 130 °C followed by one night at 40 °C).

Base	Concentration	*AI* (%)
NH_4OH	1 M	66 ± 5
	4 M	68 ± 5
	10 M	69 ± 5
NaOH	1 M	66 ± 5
	4 M	54 ± 5
	10 M	47 ± 4

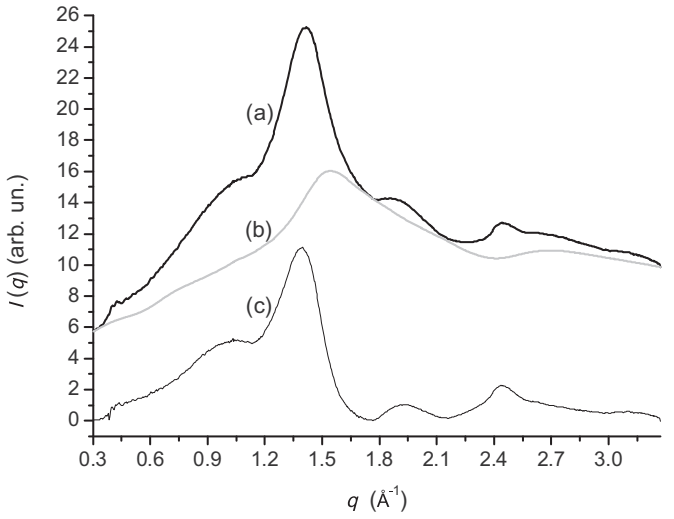

Fig. 8. Method for the determination of crystallinity indexes from WAXS pattern of chitosan fibers (radial average scattering intensity): (a) radial-averaged diffraction pattern of chitosan alcogel fibers neutralized in NaOH 1 M; (b) radial-averaged diffraction pattern of amorphous chitosan; (c) estimated crystalline contribution of chitosan fibers after subtraction of the area of the amorphous contribution, and displaying the anhydrous allomorph diffraction pattern.

anhydrous to mainly hydrated crystals depending on the neutralization conditions of the alcogels. Anhydrous chitosan is classically obtained by annealing of the sample at high temperature (*i.e.* 240 °C) (Ogawa, Hirano, Miyanishi, Yui, & Watanabe, 1984; Saito, Tabeta, & Ogawa, 1987). The degree of conversion from hydrated to anhydrous form was shown to increase with the temperature and time treatment. Another method to obtain large fractions of anhydrous allomorph consists in the treatment of chitosan in the solid state with concentrated hydrochloric acid (Osorio-Madrazo et al., 2010). Both procedures involve the production of chitosan anhydrous allomorph in a hydrophobic context but such drastic conditions (high temperature, concentrated acid) induce an important decrease of the polymer molecular weight which is not desired here to preserve good mechanical properties. The neutralization of hydroalcoholic solutions is thus an alternative to produce a large fraction of anhydrous crystals without major chitosan degradation since the molecular weight of chitosan in final fibers remains above 340,000 g/mol after the different steps of spinning process.

In addition to the anhydrous index for the semiquantitative characterization of anhydrous and hydrated allomorphs fractions, a global crystallinity index (*CI*) of chitosan fibers, including the anhydrous and hydrated allomorphs, was determined from the estimation of the contribution of an amorphous sample of chitosan (the preparation of such a sample is detailed in Section 2. WAXS). As can be seen in Fig. 8, the amorphous chitosan sample (b) did not show crystalline peaks at $q \sim 0.744$ Å^{-1} or $q \sim 1.077$ Å^{-1} respectively for the $(0\,2\,0)_h$ and $(1\,1\,0)_{an}$ diffraction reflections, but exhibited a broad halo at 2θ around 1.5 Å^{-1}. Actually, this diffractogram can be superimposed to amorphous chitosan prepared by Osorio-Madrazo et al. (2010). In order to evaluate the *CI*, the diffractogram of the amorphous was normalized to the diffractogram of semicrystalline chitosan fibers at high values of the scattering vector ($q > 3$ Å^{-1}). For each sample, the diffraction pattern of the amorphous sample was close to those of fiber samples at $q \sim 1.75$ Å^{-1} and $q \sim 2.2$ Å^{-1}. The crystalline contribution in chitosan fibers (see Fig. 8 curve c) could be deduced from the subtraction of the amorphous contribution (A_a) (Fig. 8 curve b) to the total area of the diffractograms (Fig. 8 curve a). The calculation of *CI* was thus performed from the ratio of the crystalline contribution (A_c) to the total area of the fibers diffractogram (A_{total}) (see Eq. (1)). The results are given in Table 5. Although the neutralization conditions impacted the proportion between the two allomorphs in final chitosan fibers, they did not have any significant influence on the overall crystallinity index values which were found to be close to 30% in all cases. Such values were not impacted by room temperature aging over a period up to 2 years. We also noticed that the proportion between the two allomorphs did not change with room temperature aging (results not shown).

Table 5
Area crystallinity indexes of produced chitosan fibers (C_p = 2.4% (w/w) in a 40/60 (w/w) water/1,2-propanediol medium; post-extrusion thermal treatment: 20 s at 130 °C followed by one night at 40 °C) as a function of neutralization conditions and aging at ambient atmosphere ($T = 22 \pm 2$ °C, RH = 60 ± 5%).

Neutralization conditions	Crystallinity index (%)	
	1 week	22 months
NH_4OH		
1 M	28.4 ± 2.8	28.2 ± 2.8
4 M	27.7 ± 2.8	27.9 ± 2.8
10 M	27.9 ± 2.8	28.1 ± 2.8
NaOH		
1 M	29.0 ± 2.9	28.8 ± 2.9
4 M	28.3 ± 2.8	28.2 ± 2.8
10 M	27.8 ± 2.8	27.6 ± 2.8

The possibility of preparing chitosan fibers with a high proportion in anhydrous crystals is a particularity of the spinning of hydroalcoholic chitosan solutions. Classical chitosan fibers usually exhibit a hydrated type semi-crystalline structure as reported in classical wet spinning of chitosan aqueous solutions using alkali coagulation baths (Agboh & Qin, 1997; Lee et al., 2007). A mixture of both hydrated (in higher proportion) and anhydrous allomorphs was observed by Notin, Viton, David, et al. (2006) while producing chitosan fibers by coagulation of aqueous chitosan acetate solutions in ammonia vapors. In fact, the formation of the anhydrous allomorph was mainly occurring during the post-production step: aging induced ammonium acetate salt hydrolysis leading to an increase of crystallinity but with a significant decrease of the polymer molecular weight, altering the long term mechanical properties of final fibers. In the present study, the spinning of hydroalcoholic solutions through the formation of an alcogel fiber led to the formation of anhydrous crystals after neutralization and no evolution of crystallinity with the time storage was observed up to 2 years. As fibers are free of residual salts after washings, the mechanism involved in the anhydrous form production seems to be different from Notin and could result from specific crystallization conditions in alcoholic media which constitutes a relatively hydrophobic environment for the chitosan chains.

3.4.2. *Influence of the alcohol nature*

The crystalline microstructure of chitosan fibers was also studied as a function of the nature of the alcohol used for the gelation. Fig. 9a and b shows the diffraction patterns of the fibers neutralized in NaOH 1 M and NaOH 10 M, respectively. The diffraction profiles obtained with fibers neutralized in ammonium hydroxide are, whatever the concentration in NH_4OH (1 M or 10 M), very similar to those observed for NaOH 1 M and are then not presented. In all cases, the crystallinity index value in resulting fibers was found to be close to 30%. Moreover, whatever the alcohol tested, the same transition from mainly anhydrous crystals to mainly hydrated crystals was observed on increasing the NaOH concentration (Fig. 9c). In the case of 1,3-propanediol, we noticed that the diffraction peak at $q \sim 1.077$ Å^{-1} corresponding to $(1\,1\,0)_{an}$ reflexion is better defined with a thinner profile. Clearly, the formation of larger or less defective anhydrous crystals is favored with 1,3-propanediol. The reason for such a behavior is not known, but it could result from specific interactions between 1,3-propanediol and chitosan: the

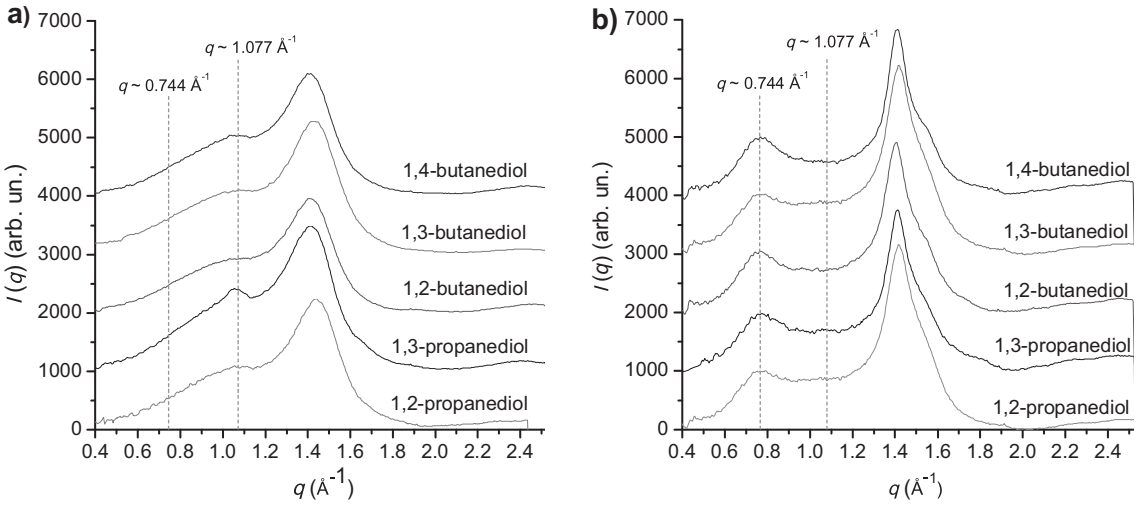

c)

	AI (%)	
	NaOH 1M	NaOH 10M
1,2-propanediol	66 ± 5	47 ± 4
1,3-propanediol	69 ± 5	42 ± 3
1,2-butanediol	65 ± 5	41 ± 3
1,3-butanediol	63 ± 5	46 ± 4
1,4-butanediol	67 ± 5	37 ± 3

Fig. 9. Influence of the alcohol structure on the crystalline microstructure of chitosan fibers (initial spinning dope: 2.4% of chitosan in a 40/60 (w/w) water/alcohol mixture; post-extrusion thermal treatment: 20 s at 130 °C followed by one night at 40 °C). (a) Diffraction patterns (average at $\varphi = 90$ and $-90°$, amorphous halo subtracted) of fibers neutralized in NaOH 1 M, (b) diffraction patterns of fibers neutralized in NaOH 10 M, (c) corresponding anhydrous index values. Scattered intensity profiles were vertically shifted by 1000 arb. un. for clarity.

exact molecular origin of which are not in the scope of this paper. The alcohol could promote crystallization by the establishment of inter-chain junctions through H-bond or solvophobic interactions. The strength of 1,3-propanediol–chitosan interactions could have reached an optimum balance: 1,3-propanediol needs to be removed in order to form anhydrous chitosan crystals, but should also previously interact with chitosan chains to yield a hydrophobic environment and exclude water from the chains.

3.4.3. *Influence of the post-extrusion thermal treatment*

Different evaporation conditions (*i.e.* different drying temperatures and times) were applied on alcogel fibers (obtained from the standard chitosan dope) before their neutralization in alkali medium. In order to better understand the formation of the semicrystalline morphology, we also decided to produce fibers by direct neutralization of the extruded hydroalcoholic chitosan solution in alkali medium, *i.e.* without post-extrusion thermal treatment, by immersion of the spinneret in the coagulation bath ("direct neutralization route").

The diffraction patterns of the resulting fibers neutralized in NaOH at different concentrations are presented in Fig. 10a.

The corresponding anhydrous index values are gathered in Fig. 1b. Whatever the nature and the concentration of the base, we noticed that the fraction of anhydrous crystals increased with the evaporation time. This evolution is related to the decrease of the water content in the alcogel fiber and the promotion of hydrophobic interactions (*i.e.* chitosan/chitosan and chitosan/alcohol interactions *vs* chitosan/water interactions). Consequently, at the neutralization step, the chitosan chains would be in a more hydrophobic environment favoring the polymer crystallization under the anhydrous form. For all neutralization conditions, the same transitions of crystalline morphology from anhydrous to hydrated allomorphs were observed on increasing the NaOH concentration, while the NH_4OH concentration did not significantly impact the allomorph composition. A maximum value of anhydrous index was found for the driest systems neutralized in NaOH 1 M or in NH_4OH. With a numerical value of *AI* above 65%, the fibers contain a dominant fraction of anhydrous allomorph.

When the drying post-extrusion thermal treatment is applied, the polymer chains are part of an alcogel network and their mobility is then strongly reduced. On the contrary, when the extruded hydroalcoholic chitosan solution is directly neutralized in an alkali bath, the neutralization occurs in the liquid polymer solution. This mobility gain could promote crystallization, but as shown in Table 6, whatever the composition of the neutralization bath, the crystallinity index values could not be significantly improved by solution crystallization. Moreover, the apparent width L_{hkl} of

Table 6
Crystallinity index values of chitosan fibers as a function of neutralization conditions obtained for different evaporation conditions: (t_0) no post-extrusion thermal treatment; (t_3): 20 s at 130 °C and 12 h at 40 °C (±3 °C).

	CI (%)	
	t_0	t_3
NaOH		
10 M	29.7 ± 3.0	27.8 ± 2.8
4 M	27.1 ± 2.7	28.3 ± 2.8
1 M	26.7 ± 2.7	29.0 ± 2.9
NH_4OH		
10 M	25.8 ± 2.6	27.9 ± 2.6
4 M	27.7 ± 2.8	27.7 ± 2.8
1 M	27.1 ± 2.7	28.4 ± 2.8

(a)

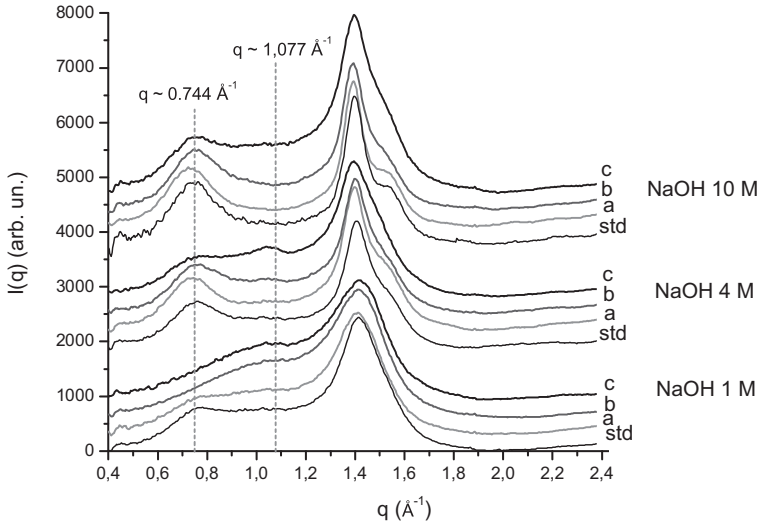

(b)

	NaOH			NH_4OH		
Evaporation conditions	1M	4M	10M	1M	4M	10M
std	50 ± 4	38 ± 3	24 ± 2	50 ± 4	52 ± 4	54 ± 4
a	55 ± 6	35 ± 3	23 ± 2	55 ± 4	56 ± 4	57 ± 4
b	66 ± 5	41 ± 3	30 ± 2	65 ± 5	65 ± 5	67 ± 5
c	66 ± 5	54 ± 4	47 ± 4	66 ± 5	68 ± 5	69 ± 5

Fig. 10. Influence of the evaporation conditions on the crystalline microstructure of fibers obtained by alcogel spinning (initial spinning dope: 2.4% of chitosan in a 40/60 (w/w) water/1,2-propanediol mixture): (a) 20 s at 130 °C (±5 °C); (b) 20 s at 130 °C and 10 min at 40 °C (±3 °C); (c) 20 s at 130 °C and 12 h at 40 °C (±3 °C); (std) direct extrusion of the hydroalcoholic dope into the alkaline coagulation bath without drying thermal treatment. Average WAXS patterns at $\varphi = 90°$ and $\varphi = -90$ °C after subtraction of the amorphous contribution. Scattering curves were vertically shifted for clarity. (b) Anhydrous index values ($AI \pm 10\%$).

hydrated crystals could be deduced using the Scherrer equation in the case of chitosan fibers produced *via* the direct neutralization route in a NaOH 10 M bath (see Fig. 10a). Indeed, these particular experimental conditions led to a well defined $(0\,2\,0)_h$ reflection at $q \sim 0.74$ Å^{-1} from which we could determine the full width at half maximum and deduce a L_{020} value close to 31 Å. This crystallite apparent size is in the same order of magnitude as those previously reported for semicrystalline chitosan in the solid state (Osorio-Madrazo et al., 2010) or crystals in regenerated cellulose fibers (Chen et al., 2007). In the case of other neutralization conditions than NaOH 10 M, the specific diffraction peaks to hydrated and anhydrous crystals at $q \sim 0.744$ Å^{-1} and $q \sim 1.077$ Å^{-1}, respectively were too broad to be able to deduce the apparent crystallite size.

3.5. Proposed mechanism for the anhydrous allomorph formation

We previously deduced that the balance between the hydrated and anhydrous allomorphs was impacted by the hydrophobic environment at the neutralization step that triggers crystallization. In order to vary the hydrophilic/hydrophobic context, we further investigated the spinning by direct neutralization in alkali solutions of hydroalcoholic dopes with various water/1,2-propanediol ratios (from 20/80 to 100/0, w/w) for a constant polymer concentration of 2.4% (w/w). The diffraction patterns of chitosan fibers obtained with neutralization in NaOH 1 M are presented in Fig. 11a. The same trend was obtained with NH_4OH coagulation baths at all concentrations, in the 1–10 M range (results not shown). As expected, we observed that the formation of the anhydrous allomorph was favored for highly alcohol-enriched solvent media. On increasing the water content in the polymer solvent, the amount of water interacting with the chitosan chains increased and the crystallization under the hydrated form was then favored by the recruitment of these interacting water molecules. The evolution of the anhydrous index values as a function of the alcohol content in the solvent of the chitosan dope exhibited a gradual increase whatever the polymer concentration ($C_p = 2.4\%$ or 0.8%, w/w) (Fig. 11b). Furthermore, although the nature of chitosan counter-ion is known to act on the polymer hydrophily (Boucard et al., 2007; Popa-Nita, Rochas, David, & Domard, 2009), it did not impact the final crystalline morphology (Fig. 11b) and led to comparable anhydrous index values as those obtained for the acetate counter-ion in the same experimental conditions.

Hence, in the case of aqueous chitosan solutions, the polymer chains are highly hydrated promoting the formation of hydrated crystals whatever the nature and the concentration of the base. Conversely, when the solvent is enriched in alcohol, the environment of the polymer chains become more hydrophobic and the crystallization under the anhydrous form is thus favored. Thus, by interacting with chitosan chains (mainly through hydrogen bonds), the alcohol molecules could act as dehydrating agents preventing the entrapment of water molecules during the crystallite formation. The polymer chain dehydration prior to neutralization could also explain the production of anhydrous type chitosan fibers by Tamura et al. (2004). In their process, the neutralization in a dilute NaOH aqueous solution (0.8 M) was performed on a filament obtained by the extrusion of an aqueous chitosan solution in a calcium chloride (or calcium acetate) saturated water/methanol (1:1, v/v) bath. These authors suggested that the coagulation could be induced by a complex formation between the polymer and the calcium ions, but in light of the results presented here, the dehydration of the extruded liquid filament in the $CaCl_2$ bath probably explains the particular crystallization under the anhydrous form. Such a desolvation effect has been reported by Sheehan and Atkins to produce calcium hyaluronate fibers by syringing solutions of calcium hyaluronate into an alcoholic solution of $CaCl_2$ (Atkins & Sheehan, 1972). All these studies tend to confirm that the chitosan allomorph formation depends on the hydration degree of the polymer chains

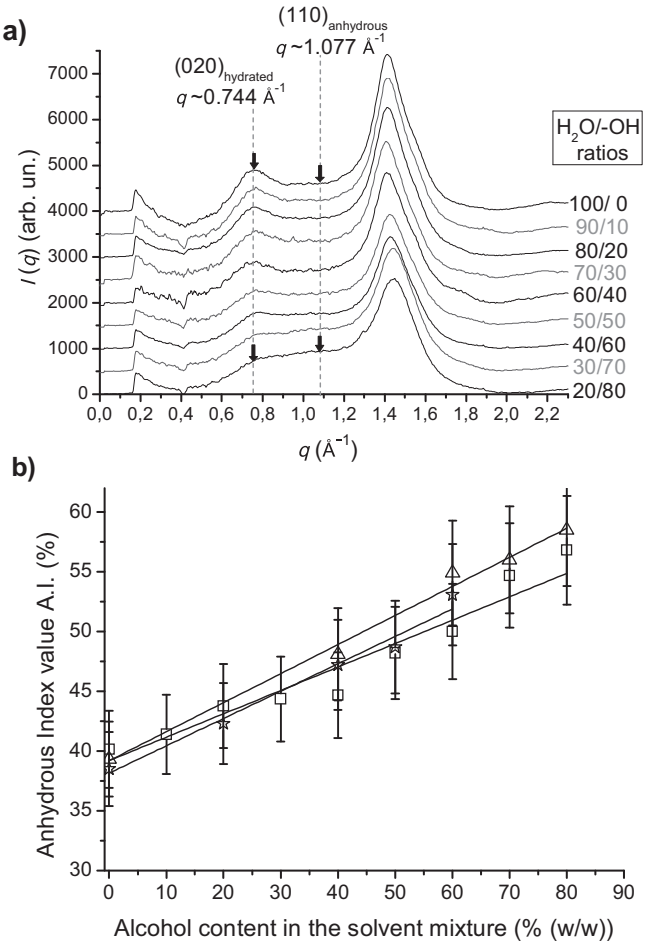

Fig. 11. Crystalline microstructure of chitosan fibers obtained by direct neutralization in a 1 M NaOH bath of hydroalcoholic chitosan acetate solutions with various water/1,2-propanediol ratios (%, w/w): (a) diffraction patterns obtained with C_p = 2.4% (w/w); (b) anhydrous index values (□) for C_p = 2.4% (w/w) and (△) for C_p = 0.8% (w/w); (☆) represents the anhydrous index values for C_p = 2.4% (w/w) in the case of chitosan hydrochloride for comparison with the acetate salt form.

when crystallization is triggered by neutralization. In this view, the influence of the alcohol nature must be interpreted through its ability to compete with water to establish interactions (mainly H-bonds) with chitosan.

The influence of the neutralization conditions on the chitosan allomorph formation is more complex. The variation of the base nature and concentration induced the formation of different anhydrous/hydrated crystalline compositions. In the case of alcogel spinning, a semi-crystalline phase containing a high proportion in anhydrous crystals was observed for the neutralization of the alcogel fibers with C_{NH_4OH} = 1 M; 4 M; 10 M and C_{NaOH} = 1 M whereas the neutralization with C_{NaOH} = 10 M induced the formation of hydrated chitosan crystals. In between, an intermediate morphology was generated by neutralization in C_{NaOH} = 4 M. Similar results were obtained after the direct neutralization of hydroalcoholic chitosan solutions (*e.g.* C_p = 2.4% in a 40/60 water/1,2-propanediol mixture). In addition, contrary to aqueous NH_4OH, the viscosity of NaOH aqueous solutions is known to increase significantly with the NaOH concentration (see Supporting Information, Table S1). Ladet, David, and Domard (2008) further studied the viscosity of the two bases in water/1,2-propanediol mixtures. While no viscosity change was observed in the case of NH_4OH, the viscosity of NaOH appeared to be significantly higher in a hydroalcoholic medium than in water. These observations could be related to specific interactions between the alcohol molecules and the Na^+;OH^- ionic species (Pu, Ng, Mok, & Chen, 2004; Von Hippel & Schleich, 1969). According to the study of Roy, Budtova, Navard, and Bedue (2001) soda hydrates consist in a "core" of $9H_2O \times$ NaOH where 9 water molecules are bound to NaOH and a "larger shell of amorphous water molecules" decreasing with the increase of soda concentration. Therefore, when the 10 M NaOH solution diffuses into the hydroalcoholic dope, the NaOH ionic species may stronger interact with the alcohol molecules and the coagulation process would start only after the NaOH–alcohol interactions equilibration. In that case, the diffusion of water molecules within the dope prior to the polymer neutralization must be considered and could explain the preferential formation of hydrated chitosan crystals. Conversely, at C_{NaOH} = 1 M, the presence of a thick layer of water molecules surrounding the NaOH core should disfavor the interactions with the alcohol leading to the quasi-instantaneous neutralization of chitosan and the formation of anhydrous crystals. Consequently, the different crystalline morphologies obtained in the final chitosan fibers must arise from different initial neutralization kinetics resulting from a competition between the diffusion kinetics of the coagulant species and the rehydration of the chains by the diffusion of water molecules into the filament during the neutralization process.

4. Conclusions

We investigated the spinning of hydroalcoholic chitosan solutions. Different post-extrusion thermal treatments were studied. After neutralization in alkali media, washings in water and drying, the resulting chitosan fibers only contain chitosan and residual physisorbed water (~10%, w/w). Contrary to standard wet-spinning of chitosan aqueous solutions, fibers produced by spinning of hydroalcoholic chitosan dopes exhibited a large proportion in anhydrous crystals. The crystallization of chitosan under anhydrous form was related to a particular physicochemical neutralization context in hydrophobic conditions. The crystalline morphology was shown to be controlled by the degree of hydration of chitosan chains when crystallization occurs. This degree of hydration mainly depends on the alcohol content in the chitosan solution or in the alcogel filament at the neutralization step as well as the competition between the neutralization kinetics on one hand and the polymer re-hydration kinetics on the other hand. The processing of hydroalcoholic chitosan solutions constitutes an alternative method to predominantly produce anhydrous allomorph without significant degradation of the polymer as in classical annealing method under drastic conditions. The characterization of the mechanical and structural properties of such anhydrous crystalline fibers is on going and will be discussed elsewhere.

Acknowledgements

This work was financially supported by Tetra Medical, the ANRT, and the FUI program MATBIOTEX. We thank Mahtani Chitosan for the gift of chitosan samples. We also thank C. Rochas for the experiments on the D2AM beamline at the European Synchrotron X-ray Facility of Grenoble (France) and Philippe Cassagnau for our discussions about the rheological aspects.

Appendix A. Supplementary data

Supplementary data associated with this article can be found, in the online version, at http://dx.doi.org/10.1016/j.carbpol.2013.04.070.

References

Abdou, E. S., Nagy, K. S. A., & Elsabee, M. Z. (2008). Extraction and characterization of chitin and chitosan from local sources. *Bioresource Technology*, *99*, 1359–1367.

Agboh, O. C., & Qin, Y. (1997). Chitin and chitosan fibers. *Polymers for Advanced Technologies*, *8*, 355–365.

Araiza, R. N. R., Rochas, C., David, L., & Domard, A. (2008). Interrupted wet-spinning process for chitosan hollow fiber elaboration. *Macromolecular Symposia*, *266*, 1–5.

Atkins, E. D. T., & Sheehan, J. K. (1972). Structure for hyaluronic-acid. *Nature: New Biology*, *235*, 253–254.

Binias, D., Boryniec, S., & Binias, W. (2005). Studies of the structure of polysaccharides in the process of alkaline treatment of dibutyrylchitin fibres. *Fibres & Textiles in Eastern Europe*, *13*, 137–140.

Blanchemain, N., Laurent, T., Chai, F., Neut, C., Haulon, S., Krump-Konvalinkova, V., et al. (2008). Polyester vascular prostheses coated with a cyclodextrin polymer and activated with antibiotics: Cytotoxicity and microbiological evaluation. *Acta Biomaterialia*, *4*, 1725–1733.

Boateng, J. S., Matthews, K. H., Stevens, H. N. E., & Eccleston, G. M. (2008). Wound healing dressings and drug delivery systems: A review. *Journal of Pharmaceutical Sciences*, *97*, 2892–2923.

Boucard, N., David, L., Rochas, C., Montembault, A., Viton, C., & Domard, A. (2007). Polyelectrolyte microstructure in chitosan aqueous and alcohol solutions. *Biomacromolecules*, *8*, 1209–1217.

Boucard, N., Viton, C., & Domard, A. (2005). New aspects of the formation of physical hydrogels of chitosan in a hydroalcoholic medium. *Biomacromolecules*, *6*, 3227–3237.

Burger, J. W. A., Halm, J. A., Wijsmuller, A. R., ten Raa, S., & Jeekel, J. (2006). Evaluation of new prosthetic meshes for ventral hernia repair. *Surgical Endoscopy and Other Interventional Techniques*, *20*, 1320–1325.

Calero, N., Munoz, J., Ramirez, P., & Guerrero, A. (2010). Flow behaviour, linear viscoelasticity and surface properties of chitosan aqueous solutions. *Food Hydrocolloids*, *24*, 659–666.

Chen, W. Y. J., & Abatangelo, G. (1999). Functions of hyaluronan in wound repair. *Wound Repair and Regeneration*, *7*, 79–89.

Chen, X., Burger, C., Wan, F., Zhang, J., Rong, L. X., Hsiao, B. S., et al. (2007). Structure study of cellulose fibers wet-spun from environmentally friendly NaOH/urea aqueous solutions. *Biomacromolecules*, *8*, 1918–1926.

Cho, J. Y., Heuzey, M. C., Begin, A., & Carreau, P. J. (2006). Viscoelastic properties of chitosan solutions: Effect of concentration and ionic strength. *Journal of Food Engineering*, *74*, 500–515.

Demargerandre, S., & Domard, A. (1994). Chitosan carboxylic-acid salts in solution and in the solid-state. *Carbohydrate Polymers*, *23*, 211–219.

Desbrieres, J. (2002). Viscosity of semiflexible chitosan solutions: Influence of concentration, temperature, and role of intermolecular interactions. *Biomacromolecules*, *3*, 342–349.

Domard, A., & Domard, M. (2002). Structure-properties relationship and biomedical applications. In S. Dumitriu (Ed.), *Polymeric biomaterials* (2nd ed., pp. 187–212). Marcel Dekker: New York.

Earle, D., & Romanelli, J. (2007). Prosthetic materials for hernia: What's new. *Contemporary Surgery*, *63*, 63–69.

East, G. C., & Qin, Y. M. (1993). Wet spinning of chitosan and the acetylation of chitosan fibers. *Journal of Applied Polymer Science*, *50*, 1773–1779.

El-Tahlaway, K., & Hudson, S. M. (2006). Chitosan: Aspects of fiber spinnability. *Journal of Applied Polymer Science*, *100*, 1162–1168.

Focher, B., Beltrame, P. L., Naggi, A., & Torri, G. (1990). Alkaline N-deacetylation of chitin enhanced by flash treatments – Reaction-kinetics and structure modifications. *Carbohydrate Polymers*, *12*, 405–418.

Havrilia, S., & Negami, S. (1967). A complex plane representation of dielectric and mechanical relaxation processes in some polymers. *Polymer*, *8*, 161–210.

Hudson, S. M. (1998). Applications of chitin and chitosan as fiber and textile chemicals. In A. Domard, G. A. F. Roberts, & K. M. Varum (Eds.), *Advances in chitin science II* (pp. 590–599). Lyon: Jacques Andre Publisher.

Ibanes, C., David, L., De Boissieu, M., Seguela, R., Epicier, T., & Robert, G. (2004). Structure and mechanical behavior of nylon-6 fibers filled with organic and mineral nanoparticles. I. *Journal of Polymer Science Part B: Polymer Physics*, *42*, 3876–3892.

Jayakumar, R., Prabaharan, M., Kumar, P. T. S., Nair, S. V., & Tamura, H. (2011). Biomaterials based on chitin and chitosan in wound dressing applications. *Biotechnology Advances*, *29*, 322–337.

Knaul, J. Z., & Creber, K. A. M. (1997). Coagulation rate studies of spinnable chitosan solutions. *Journal of Applied Polymer Science*, *66*, 117–127.

Knaul, J. Z., Hudson, S. M., & Creber, K. A. M. (1999a). Improved mechanical properties of chitosan fibers. *Journal of Applied Polymer Science*, *72*, 1721–1732.

Knaul, J. Z., Hudson, S. M., & Creber, K. A. M. (1999b). Crosslinking of chitosan fibers with dialdehydes: Proposal of a new reaction mechanism. *Journal of Polymer Science Part B: Polymer Physics*, *37*, 1079–1094.

Ladet, S., David, L., & Domard, A. (2008). Multi-membrane hydrogels. *Nature*, *452*, 76–79.

Lee, K. Y., Jeong, L., Kang, Y. O., Lee, S. J., & Park, W. H. (2009). Electrospinning of polysaccharides for regenerative medicine. *Advanced Drug Delivery Reviews*, *61*, 1020–1032.

Lee, S. H., Kim, Y., & Kim, Y. (2007). Effect of the concentration of sodium acetate (SA) on crosslinking of chitosan fiber by epichlorohydrin (ECH) in a wet spinning system. *Carbohydrate Polymers*, *70*, 53–60.

Lide, D. R. (2010). *Handbook of chemistry & physics*. Florida, USA: CRC Press.

Martinez, A., Chornet, E., & Rodrigue, D. (2004). Steady-shear rheology of concentrated chitosan solutions. *Journal of Texture Studies*, *35*, 53–74.

McKinley, G. H. (2005). Dimensionless groups for understanding free surface flows of complex fluid. *The Society of Rheology [SOR]. Rheology Bulletin*, *74*, 6–10.

Meaume, S., Vallet, D., Morere, M. N., & Teot, L. (2005). Evaluation of a silver-releasing hydroalginate dressing in chronic wounds with signs of local infection. *Journal of Wound Care*, *14*, 411–419.

Merkovich, E. A., Carruette, M. L., Babak, V. G., Vikhoreva, G. A., Gal'braikh, L. S., & Kim, V. E. (2001). Kinetics of the initial stage of gelation in chitosan solutions containing glutaric aldehyde: Viscometric study. *Colloid Journal*, *63*, 350–354.

Meyer, M., Baltzer, H., & Schwikal, K. (2010). Collagen fibres by thermoplastic and wet spinning. *Materials Science & Engineering C: Materials for Biological Applications*, *30*, 1266–1271.

Min, B. M., Jeong, L., Nam, Y. S., Kim, J. M., Kim, J. Y., & Park, W. H. (2004). Formation of silk fibroin matrices with different texture and its cellular response to normal human keratinocytes. *International Journal of Biological Macromolecules*, *34*, 281–288.

Molloy, R. (2002). Effects of some processing variables in the wet-spinning of chitosan monofilament fibres. In K. Suchiva, S. Chandrkrachang, P. Methacanon, & M. G. Peter (Eds.), *Advances in chitin sciences* (Vol. V) (pp. 207–211). Bangkok: National Metals and Materials Center.

Montembault, A., Viton, C., & Domard, A. (2005a). Rheometric study of the gelation of chitosan in aqueous solution without cross-linking agent. *Biomacromolecules*, *6*, 653–662.

Montembault, A., Viton, C., & Domard, A. (2005b). Physico-chemical studies of the gelation of chitosan in a hydroalcoholic medium. *Biomaterials*, *26*, 933–943.

Montembault, A., Viton, C., & Domard, A. (2005c). Rheometric study of the gelation of chitosan in a hydroalcoholic medium. *Biomaterials*, *26*, 1633–1643.

Mucha, M. (1997). Rheological characteristics of semi-dilute chitosan solutions. *Macromolecular Chemistry and Physics*, *198*, 471–484.

Muzzarelli, R. A. A. (2009). Chitins and chitosans for the repair of wounded skin, nerve, cartilage and bone. *Carbohydrate Polymers*, *76*, 167–182.

Notin, L., Viton, C., David, L., Alcouffe, P., Rochas, C., & Domard, A. (2006). Morphology and mechanical properties of chitosan fibers obtained by gel-spinning: Influence of the dry-jet-stretching step and ageing. *Acta Biomaterialia*, *2*, 387–402.

Notin, L., Viton, C., Lucas, J. M., & Domard, A. (2006). Pseudo-dry-spinning of chitosan. *Acta Biomaterialia*, *2*, 297–311.

Ogawa, K., Hirano, S., Miyanishi, T., Yui, T., & Watanabe, T. (1984). A new polymorph of chitosan. *Macromolecules*, *17*, 973–975.

Okuyama, K., Noguchi, K., Miyazawa, T., Yui, T., & Ogawa, K. (1997). Molecular and crystal structure of hydrated chitosan. *Macromolecules*, *30*, 5849–5855.

Osman, Z. (2005). Thermal and conductivity studies of chitosan acetate-based polymer electrolytes. *Ionics*, *11*, 397–401.

Osorio-Madrazo, A., David, L., Trombotto, S., Lucas, J. M., Peniche-Covas, C., & Domard, A. (2010). Kinetics study of the solid-state acid hydrolysis of chitosan: Evolution of the crystallinity and macromolecular structure. *Biomacromolecules*, *11*, 1376–1386.

Parenteau-Bareil, R., Gauvin, R., & Berthod, F. (2010). Collagen-based biomaterials for tissue engineering applications. *Materials*, *3*, 1863–1887.

Peters, R. H. (1963). *Textile chemistry. The chemistry of fibres* (Vol. 1) Amsterdam–London–New York: Elsevier Publishing Co.

Pillai, C. K. S., & Sharma, C. P. (2009). Electrospinning of chitin and chitosan nanofibres. *Trends in Biomaterials & Artificial Organs*, *22*, 179–201.

Popa-Nita, S., Rochas, C., David, L., & Domard, A. (2009). Structure of natural polyelectrolyte solutions: Role of the hydrophilic/hydrophobic interaction balance. *Langmuir*, *25*, 6460–6468.

Popa-Nita, S., Alcouffe, P., Rochas, C., David, L., & Domard, A. (2010). Continuum of structural organization from chitosan solutions to derived physical forms. *Biomacromolecules*, *11*, 6–12.

Pu, Q., Ng, S., Mok, V., & Chen, S. B. (2004). Ion bridging effects on the electroviscosity of flexible polyelectrolytes. *Journal of Physical Chemistry B*, *108*, 14124–14129.

Puolakkainen, P. A., Twardzik, D. R., Ranchalis, J. E., Pankey, S. C., Reed, M. J., & Gombotz, W. R. (1995). The enhancement in wound-healing by transforming growth-factor-beta (1) (TGF-beta (1)) depends on the topical delivery system. *Journal of Surgical Research*, *58*, 321–329.

Qin, Y. M. (2008). Alginate fibres: An overview of the production processes and applications in wound management. *Polymer International*, *57*, 171–180.

Quijada-Garrido, I., Iglesias-Gonzalez, V., Mazon-Arechederra, J. M., & Barrales-Rienda, J. M. (2007). The role played by the interactions of small molecules with chitosan and their transition temperatures. Glass-forming liquids: 1,2,3-Propanetriol (glycerol). *Carbohydrate Polymers*, *68*, 173–186.

Rathke, T. D., & Hudson, S. M. (1994). Review of chitin and chitosan as fiber and film formers. *Journal of Macromolecular Science: Reviews in Macromolecular Chemistry and Physics*, *C34*, 375–437.

Ravikumar, M. N. V. (1999). Chitin and chitosan fibres: A review. *Bulletin of Materials Science*, *22*, 905–915.

Ravindra, S., Mohan, Y. M., Reddy, N. N., & Raju, K. M. (2010). Fabrication of antibacterial cotton fibres loaded with silver nanoparticles via green approach. *Colloids and Surfaces A: Physicochemical and Engineering Aspects*, *367*, 31–40.

Roberts, G. A. F. (1992). *Chitin chemistry*. London: Macmillan Press Ltd.

Robitzer, M., David, L., Rochas, C., Di Renzo, F., & Quignard, F. (2008). Nanostructure of calcium alginate aerogels obtained from multistep solvent exchange route. *Langmuir*, *24*, 12547–12552.

Roy, C., Budtova, T., Navard, P., & Bedue, O. (2001). Structure of cellulose-soda solutions at low temperatures. *Biomacromolecules*, *2*, 687–693.

Saito, H., Tabeta, R., & Ogawa, K. (1987). High-resolution solid-state C-13 NMR-study of chitosan and its salts with acids – Conformational characterization of polymorphs and helical structures as viewed from the conformation-dependent C-13 chemical-shifts. *Macromolecules*, *20*, 2424–2430.

Schneider, A., Wang, X. Y., Kaplan, D. L., Garlick, J. A., & Egles, C. (2009). Biofunctionalized electrospun silk mats as a topical bioactive dressing for accelerated wound heating. *Acta Biomaterialia*, *5*, 2570–2578.

Serrero, A., Trombotto, S., Cassagnau, P., Bayon, Y., Gravagna, P., Montanari, S., et al. (2010). Polysaccharide gels based on chitosan and modified starch: Structural characterization and linear viscoelastic behavior. *Biomacromolecules*, *11*, 1534–1543.

Tamura, H., Tsuruta, Y., Itoyama, K., Worakitkanchanakul, W., Rujiravanit, R., & Tokura, S. (2004). Preparation of chitosan filament applying new coagulation system. *Carbohydrate Polymers*, *56*, 205–211.

Toffey, A., & Glasser, W. G. (1999). Chitin derivatives. II. Time–temperature-transformation cure diagrams of the chitosan amidization process. *Journal of Applied Polymer Science*, *73*, 1879–1889.

Tomihata, K., & Ikada, Y. (1997). In vitro and in vivo degradation of films of chitin and its deacetylated derivatives. *Biomaterials*, *18*, 567–575.

Vårum, K. M., Ottøy, M. H., & Smidsrød, O. (1994). Water-solubility of partially N-acetylated chitosans as a function of ph: effect of chemical composition and depolymerisation. *Carbohydrate Polymers*, *25*, 65–70.

Von Hippel, P. H., & Schleich, T. (1969). Ions effect on the solution of biological macromolecules. *Accounts of Chemical Research*, *2*, 257–265.

Wang, X. F., Um, I. C., Fang, D. F., Okamoto, A., Hsiao, B. S., & Chu, B. (2005). Formation of water-resistant hyaluronic acid nanofibers by blowing-assisted electro-spinning and non-toxic post treatments. *Polymer*, *46*, 4853–4867.

Wei, Y. C., Hudson, S. M., Mayer, J. M., & Kaplan, D. L. (1992). *Journal of Polymer Science Part A: Polymer Chemistry*, *30*, 2187–2193.

Woodings, C., & The Textile Institute. (2001). *Regenerated cellulose fibres*. UK: Woodhead Publishing Ltd.

Yang, Q., Dou, F. D., Liang, B. R., & Shen, Q. (2005). Studies of cross-linking reaction on chitosan fiber with glyoxal. *Carbohydrate Polymers*, *59*, 205–210.

Yui, T., Imada, K., Okuyama, K., Obata, Y., Suzuki, K., & Ogawa, K. (1994). Molecular and crystal-structure of the anhydrous form of chitosan. *Macromolecules*, *27*, 7601–7605.

Ziabicki, A. (1976). . *Fundamental studies of fibre formation* (Vol. 3) Minnesota: John Wiley & Sons Ltd.